CHINESE OPTICS LETTERS

Vol. 23, No. 1 | January 2025

White-light cavity and mode splitting effect in a three-turn lossy microfiber coil resonator

Feilin Zhang (张飞麟), Xiyuan Chen (陈熙源)*, Yulu Zhong (钟雨露), Qixuan Li (李启轩), and Mengmeng Sha (沙梦梦)

Key Laboratory of Micro-Inertial Instrument and Advanced Navigation Technology, Ministry of Education, School of Instrument Science and Engineering, Southeast University, Nanjing 210096, China

*Corresponding author: chxiyuan@seu.edu.cn

Received June 27, 2024 | Accepted July 24, 2024 | Posted Online February 4, 2025

Under a specified loss condition, the resonant mode in a three-turn lossy microfiber coil resonator exhibits periodic evolution among normal resonance, white-light cavity effect, and resonance mode splitting in response to alterations in the phase shift and coupling state. It exhibits normal resonance when the coupling state exceeds a threshold with specific loss. The white-light cavity effect is activated when the coupling state matches loss. The resonant phase bifurcates as the coupling state falls below the threshold. The excitation conditions for each resonant mode have been derived, and the critical coupling conditions exist for both normal resonance and mode splitting in the case of relatively small losses.

Keywords: white-light cavity effect; mode splitting; microfiber coil resonator.

DOI: 10.3788/COL202523.012601

1. Introduction

A three-dimensional resonator, referred to as a microfiber coil resonator (MCR), is prepared by tightly wrapping a microfiber around a supporting rod featuring a lower refractive index[1–3]. This particular configuration enables efficient interturn coupling transmission and resonant excitation by harnessing the significant evanescent field properties of the microfiber[4–6]. Due to the pervasive coupling effect throughout the entire structure, its resonant modes demonstrate an exceptionally high sensitivity to the coupling condition[7–9]. The exceptional optical properties and low manufacturing cost of the MCR make it a highly promising optical device for various applications in nonlinear optics, optical sensing, optical amplification, and quantum computing[10–12]. While numerous scholars have conducted extensive research on the MCR using experimental and simulation methods, certain unknown factors have hindered its practical application and broader acceptance[13–15].

In an MCR with only two turns, the light propagates through interturn coupling between adjacent two turns of microfibers, similar to the behavior observed in a directional coupler[16]. It resembles a single-ring resonant cavity in which the entire ring is located within the coupling region. Thus, they display comparable resonant behaviors. For an MCR with more than two turns, the complex multimode interference is excited due to the presence of more propagation modes, leading to a potential obscuring of their resonant characteristics. A previous study has revealed that the regularity of the spectral distribution with respect to the coupled state for the MCR with more than three turns ceases to exist, while the dependence of the resonant behavior of the MCR with three turns on the coupled condition is still somewhat periodic[17]. However, the intuitive explanation of the periodicity has not been found[18]. What is more, the current analysis is restricted to the group delay expansion of lossless MCR, and the dependence of periodicity on the coupling and loss conditions has not yet been fully established. In practice, losses have significant implications for the resonance modes of the MCR and cannot be ignored.

Remarkably, the periodicity of the MCR with three turns has been unraveled in the work of this Letter. The resonance mode undergoes periodic transitions among normal resonance, white-light cavity (WLC) effect, and resonance splitting in response to the coupling conditions. In general, the WLC effect, initially conceived for gravitational wave detection, can be stimulated by placing a suitable medium in the resonator with which to counteract the variation of wavelength with frequency[19,20]. During the occurrence of the WLC effect, the transmission phase accumulated in a roundtrip becomes frequency-independent, allowing for a wide-band resonance to be excited simultaneously[21]. On the other hand, the resonance splitting, which can be applied to a self-referential sensing scheme, is realized by introducing two or more coupled identical modes into a system[22–24]. Thanks to the special coupling-dominated resonance mode of the MCR and the advantage of post-tuning capability of the MCR, it is possible to realize the WLC effect and resonance splitting in a passive MCR with the assistance of precise microfabrication and thermal control techniques. It should be pointed out that these resonant modes

may also present in an MCR with more than three turns. However, the spectral behavior of the MCR with more than three turns lacks periodicity, which makes it difficult to obtain analytical solutions for the WLC effect and resonance splitting.

In this Letter, two types of loss conditions are assumed to explore the periodic evolution of the resonant mode in a three-turn MCR by means of numerical modeling. The first type involves a low-loss condition, which is the achievable level of the microfiber preparation process at present. The second type refers to a special threshold loss value, under which the critical coupling states of normal resonance and mode splitting coincide with the condition of the white-light cavity effect. The excitation conditions of these resonant modes are all derived, and the characteristics of each mode have also been discussed. These inferences contribute to the refinement of the theory of light transmission in an MCR and promote its implementation in practical applications.

2. Transmission Function of an MCR with Three Turns

Let us start with the transmission function of a three-turn MCR. The schematic of a three-turn MCR is shown in Fig. 1, where n_1 and n_2 denote the refractive indices of the microfiber and its surrounding medium, respectively. The diameter of the microfiber is of the same order of magnitude as the radiation wavelength, leading to the generation of self-coupling between co-propagating lights in adjacent turns of the microfiber coil with a suitable pitch[25]. What is more, the length of each coil is assumed to be L, which greatly exceeds the diameter of the microfiber. As a result, the adiabatic approximation of parallel transport is a suitable method to apply to an MCR due to the significantly smaller transversal dimension of the propagating mode in the microfiber compared to the characteristic bend radius in practical applications[26]. In our analysis, the length and pitch of each turn within the MCR are assumed to be uniform, and only one polarization mode is considered. Therefore, the coupling strength between adjacent microfibers are uniformly equal across the entire MCR, and the difference in propagation constants between different circles is ignored. Practically, L is much larger than the microfiber diameter. Thus, the transmission model can be analyzed by the adiabatic approximation of parallel transport.

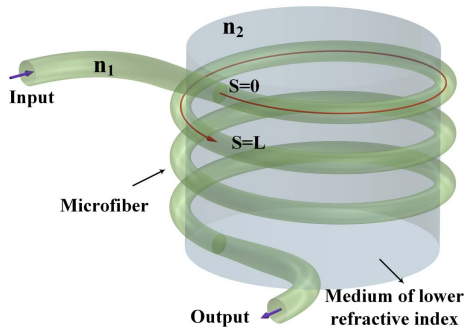

Fig. 1. Schematic of a three-turn MCR.

The transmission of light in a three-turn MCR can be described by three coupled mode equations[27],

$$\begin{cases} \frac{dA_1(s)}{ds} = ikA_2(s) - \alpha A_1(s) \\ \frac{dA_2(s)}{ds} = ikA_1(s) + ikA_3(s) - \alpha A_2(s) \\ \frac{dA_3(s)}{ds} = ikA_2(s) - \alpha A_3(s) \end{cases}, \tag{1}$$

where $A(s)$ is the varying amplitude of the optical field in one of the coils at a distance s around the coil, k is the coupling coefficient between two adjacent microfibers, and α is the loss coefficient of the microfiber. Considering the continuous spiral structure of the MCR in its geometry, the boundary conditions can be described by the relationship that the input of the previous turn is equivalent to the output of the next turn: $A_1(0) = A_0, A_2(0) = A_1(L)e^{i\varphi_0}$, and $A_3(0) = A_2(L)e^{i\varphi_0}$, where A_0 is the input optical amplitude and $\varphi_0 = \beta L$ is the one round trip phase shift, in which β is the propagation constant. As a result, the transmission coefficient can be obtained and simplified into the following form by solving this differential equation system:

$$\begin{aligned} T &= |T|e^{i\varphi_T} = \frac{A_3(L)e^{i\varphi_0}}{A_0} \\ &= \frac{\gamma\left[i2\sqrt{2}\gamma e^{i\varphi_0}\sin\left(\sqrt{2}K\right) + 2\gamma^2 e^{i2\varphi_0} + \cos\left(\sqrt{2}K\right) - 1\right]}{2e^{-i\varphi_0} + \gamma^2 e^{i\varphi_0}\left[\cos\left(\sqrt{2}K\right) - 1\right] - i2\sqrt{2}\gamma\sin\left(\sqrt{2}K\right)}, \\ \gamma &= e^{-\alpha L}, \end{aligned} \tag{2}$$

where φ_T is the phase delay of the output, γ is the attenuation factor, and $K = k \cdot L$ is defined as the coupling parameter, and it can be as large as about 300[28].

In contrast to the convention of using $\sin(K)$ to represent the degree of coupling in the coupled mode theory[29], a coupling factor $\cos(\sqrt{2}K)$ is introduced in this Letter to characterize the coupling state in an MCR, thereby facilitating subsequent analysis. When $|\cos(\sqrt{2}K)| = 1$, it represents that the pitch between adjacent microfibers is large enough to prevent any coupling, or the input light field is completely outputted from the output end after a complete coupling cycle, resulting in ineffective coupling. Conversely, when $\cos(\sqrt{2}K) = 0$, the light field that was supposed to be coupled to the output end has coupled back to the original microfiber. The presence of the trigonometric term indicates that the distribution of transmittance is shifted with the coupling parameter in a period of $\sqrt{2}\pi$, while the complex exponential term signifies that the resonance phase is periodically shifted by 2π like any other optical resonator. Further, the light power transmittance of the system can be obtained by $P = |T|^2$.

3. Evolution of Resonance Mode Under Different Coupling and Loss Conditions

As shown in Fig. 2(a), the distribution of light power transmittance P as a function of one round trip phase shift (equivalent to a dimensionless wavelength) and coupling parameter is exhibited by assuming $\gamma = 1/(2^{1/20}) \approx 0.9659$ [$\alpha L = (\ln 2)/20 \approx 0.0347$], in which m is an integer, and the mode depth is indicated by the color bar. Obviously, the resonant mode exhibits its periodic evolution with the change of the phase shift and coupling condition.

First, the normal resonance can be excited when $\cos(\sqrt{2}K)$ exceeds a certain threshold $\cos(\sqrt{2}K_{\mathrm{WL}})$ and phase matching [the $(2m \pm 1/2)\pi$ one round trip phase shift] is satisfied. In fact, the MCR in this state exhibits similar properties to a single-ring resonator, except that the eigenmode deviates by a phase of $\pi/2$ from that of the single-ring resonator. On the other side, the degeneracy of the resonant mode is raised, and the resonant phase undergoes a bifurcation as $\cos(\sqrt{2}K)$ decreases below the threshold, resulting in the emergence of two symmetric modes. By deriving the extremum curve with respect to the one round trip phase shift, the splitting phase φ_{sp} of the eigenmode can be obtained by

$$\sin(\varphi_{\mathrm{sp}_1}) = \frac{(\gamma^2+1)\left[\cos\left(\sqrt{2}K\right)-3\right] + \sqrt{\left[(\gamma^2-1)^2 - 4\gamma^2\cos\left(\sqrt{2}K\right)\right]\left[3\cos\left(\sqrt{2}K\right)-1\right]^2}}{4\sqrt{2}\gamma\sin\left(\sqrt{2}K\right)}, \varphi_{\mathrm{sp}_2} = -(\varphi_{\mathrm{sp}_1}+\pi), \tag{3}$$

where φ_{sp_1} and φ_{sp_2} are the symmetrical two resonant modes. Finally, the threshold mentioned above can be determined by aligning the transmitted phase with the endpoints of the resonance mode splitting, namely the normal resonance phase,

$$\sqrt{2}(\gamma+\gamma^{-1}) = \cot\left(\frac{K_{\mathrm{WL}}}{\sqrt{2}}\right) \pm \sqrt{9\cos\left(\sqrt{2}K_{\mathrm{WL}}\right) - \csc\left(\frac{K_{\mathrm{WL}}}{\sqrt{2}}\right)^2 + 4\sec\left(\frac{K_{\mathrm{WL}}}{\sqrt{2}}\right)^2 - 6} + 2\tan\left(\frac{K_{\mathrm{WL}}}{\sqrt{2}}\right). \tag{4}$$

It is remarkable that the threshold corresponds to the condition that the MCR can resonate over a wide spectrum simultaneously, like a white-light cavity. Notice that the emergence of the WLC effect and mode splitting is accompanied by a non-positive $\cos(\sqrt{2}K)$. In this case, a portion of the optical field will be coupled back to the MCR and continue to participate in coupled propagation, resulting in more complex interactions among the light waves. This leads to a lift in the degeneracy of the resonant modes[30]. Thus, the observed WLC effect and mode splitting in the MCR are attributed to the complex interference effects of light propagating along the microfiber from one turn to another and then returning to the previous turn with the assistance of coupling.

For the normal resonance, a pair of critical coupling conditions can be obtained by finding the extreme values of the transmittance P at the resonant phase,

$$\sqrt{2}K_{\mathrm{cri}} = 2\arctan\left[\frac{\gamma\left(\sqrt{2}\pm\sqrt{1-\gamma^2}\right)}{1+\gamma^2}\right] + 2m\pi, \tag{5}$$

where the plus and minus signs correspond to a smaller and larger $\cos(\sqrt{2}K_{\mathrm{cri}})$ for the assumed case of $\gamma = 1/(2^{1/20})$, $\cos(\sqrt{2}K_{\mathrm{cri}_1}) = 0.5$, and $\cos(\sqrt{2}K_{\mathrm{cri}_2}) = 0.1772$, respectively. Although the transmittances of the MCR at the resonance are all zero in this pair of critical coupling states, the coupling propagation mode of the optical field in the MCR varies due to different values of $\cos(\sqrt{2}K_{\mathrm{cri}})$. When the minus sign is taken [corresponding to the larger critical coupling condition $\cos(\sqrt{2}K_{\mathrm{cri}_1})$], a narrower resonance linewidth will be obtained (with a smaller transmittance at the detuned condition). There also exists critical coupling $K_{\mathrm{cri-sp}}$ in the process of mode splitting where the transmittance is 0,

$$K_{\mathrm{cri-sp}} = 2\sqrt{2}\arctan\left(\frac{1}{\gamma}\pm\sqrt{\frac{1}{\gamma^2}-1}\right) + 2\sqrt{2}m\pi. \tag{6}$$

The plus and minus signs correspond to two symmetric coupling coefficients in a coupling period [corresponding to an equal $\cos(\sqrt{2}K_{\mathrm{cri-sp}})$] for the assumed case of $\gamma = 1/(2^{1/20})$ and $\cos(\sqrt{2}K_{\mathrm{cri-sp}}) = -0.8661$. In addition, the WLC effect condition in this case is $\cos(\sqrt{2}K_{\mathrm{WL}}) = -0.035$. Specially, it found that the smaller critical coupling condition of the normal resonance and the critical coupling condition of the mode splitting coincide with the condition of the WLC effect when the loss rises to $\gamma = 1/(2^{1/2}) \approx 0.7071$ [$\alpha L = (\ln 2)/2 \approx 0.3466$], i.e., $\cos(\sqrt{2}K_{\mathrm{cri}_2}) = \cos(\sqrt{2}K_{\mathrm{cri-sp}}) = \cos(\sqrt{2}K_{\mathrm{WL}}) = 0$. The resonant mode is dominated by the WLC effect at this point. Moreover, Eq. (6) is meaningless as the losses continue to increase, and the critical coupling for mode splitting no longer exists.

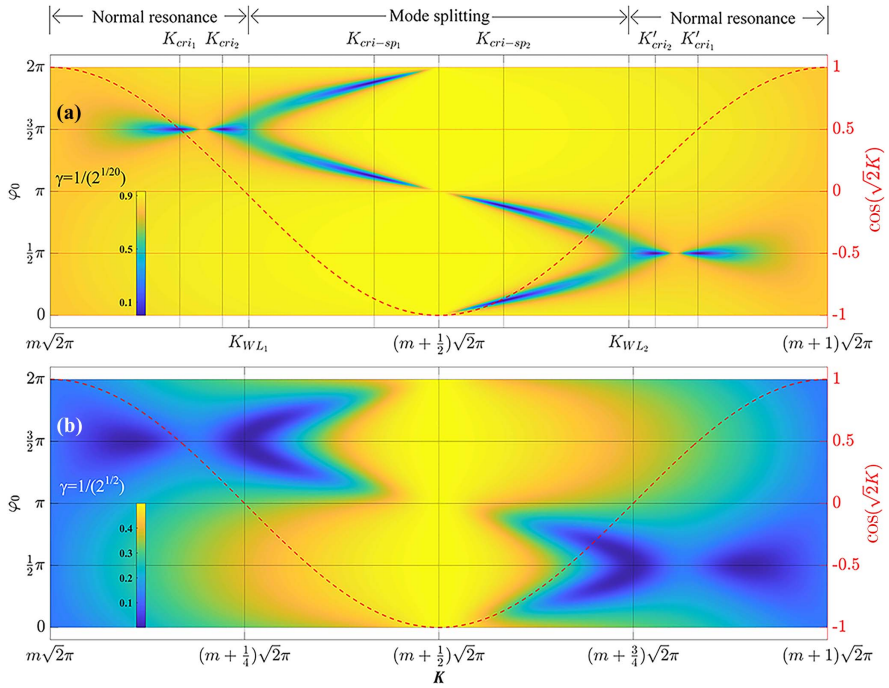

Fig. 2. Evolution of resonant modes in a three-turn MCR over a period of coupling factor $\cos(\sqrt{2}K)$ when (a) $\gamma = 1/(2^{1/20})$ and (b) $\gamma = 1/(2^{1/2})$.

The transmission spectra of different resonance modes mentioned above in a three-turn MCR at the critical coupling condition under normal resonance, the critical coupling condition under mode splitting, and the WLC effect condition when the losses are assumed to be $\gamma = 1/(2^{1/20})$ and $\gamma = 1/(2^{1/2})$ are shown in Fig. 3. Note that the transmission loss is relatively higher at the detuning of normal resonance, while in the case of detuning in resonance splitting corresponding the coupling factor $\cos(\sqrt{2}K)$ of negative value, the transmission loss is relatively minimum. This means that the effective length of the resonator is determined by the coupling condition and resonance mode.

4. Characteristics of the White-Light Cavity Effect and Mode Splitting

When $\cos(\sqrt{2}K)$ decreases to near the certain threshold at a given loss, the resonant linewidth is extended, and the transmission dip becomes flat. In this instance, a resonance mode over a broad spectrum could be observed, resembling that of a white-light cavity. As illustrated in Fig. 4, the group delay $\partial\varphi_T/\partial\omega$ demonstrates frequency-independence in the proximity of the white-light resonance mode, while the group delay dispersion $\partial^2\varphi_T/\partial\omega^2$ remains nearly zero.

In the WLC effect condition described in Eq. (4), the plus sign is operative for $-1 < \cos(\sqrt{2}K) \leq -0.0357$, whereas both plus

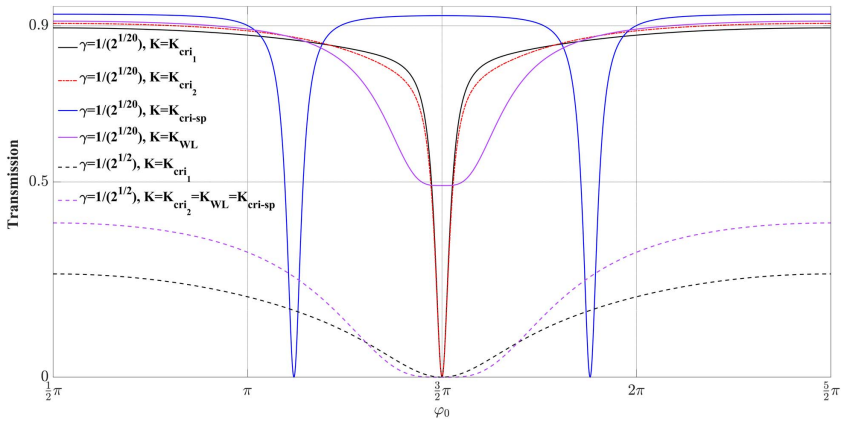

Fig. 3. Transmission spectra of different resonance modes in a three-turn MCR at different coupling conditions when $\gamma = 1/(2^{1/20})$ and $\gamma = 1/(2^{1/2})$.

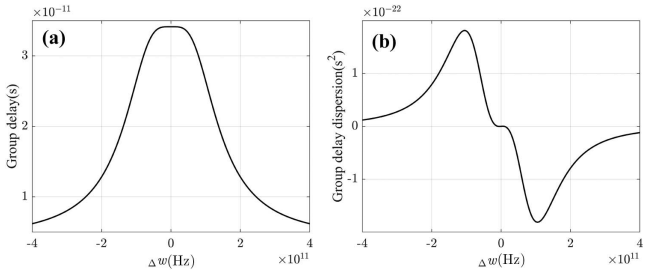

Fig. 4. (a) Group delay and (b) group delay dispersion under white-light resonant conditions.

and minus signs are operative when $-0.0357 < \cos(\sqrt{2}K) < 0$. It is evident that achieving the WLC effect entails rigorous matching conditions between coupling and loss. For a given negative coupling factor $\cos(\sqrt{2}K)$ closer to 0, there will be two relatively larger γ(lower loss) corresponding to the achievement of the white-light resonance condition, as shown in Fig. 5(a). Moreover, as the loss increases to a certain extent, the corresponding γ decreases with the decreasing $\cos(\sqrt{2}K)$.

Note that the resonance depth is relatively shallow in the case of white-light resonance, as shown in Fig. 3. Actually, the matching of loss and coupling has a profound effect on the resonance depth. Figure 5(b) shows the dependence of white-light resonance depth on different coupling conditions. In order to achieve a significant depth of resonance in the WLC effect, it is necessary to conduct the operation under conditions of coupling state $\cos(\sqrt{2}K)$ closer to 0. When the coupling state $\cos(\sqrt{2}K) = -0.02811$, the resonant depth reaches its maximum value of 0.6511, and the corresponding loss is $\gamma = 0.890566$ or $\gamma = 0.597781$. It is important to note that even though an identical resonance depth can be attained under two distinct loss conditions, their transmittance at detuning is not identical. Moreover, the results in Fig. 3 reveal that the spectral width of the WLC effect is broader for a loss of $\gamma = 1/(2^{1/2})$ compared to that of $\gamma = 1/(2^{1/20})$, implying that the spectral width of the WLC effect is susceptible to loss. Consequently, the bandwidth of the WLC effect in the frequency domain can be flexibly regulated by tuning the loss to suit specific requirements.

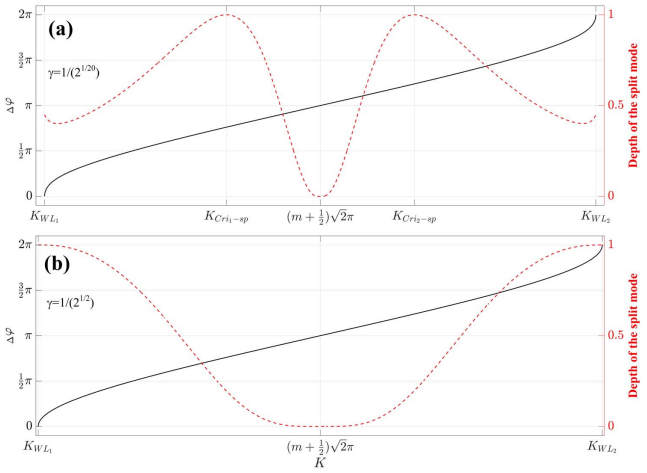

Fig. 6. The dependence of split phase difference and resonance depth of mode splitting on coupling parameter when (a) $\gamma = 1/(2^{1/20})$ and (b) $\gamma = 1/(2^{1/2})$.

When the coupling state $\cos(\sqrt{2}K)$ is below the WLC effect condition, resonance mode splitting can be observed. According to the description of the mode splitting condition in Eq. (3), the split phase difference can be expressed as $\Delta\varphi = |\varphi_{sp_1} - \varphi_{sp_2}|$. In the case of critical coupling during mode splitting described in Eq. (6), the split phase difference will be

$$\Delta\varphi_{cri} = 2\ \text{arccocos}\left\{-2\sqrt{2}\gamma(\gamma^2-1) \times \csc\left[4\arctan\left(\sqrt{\frac{1}{\gamma^2}-1}\pm\frac{1}{\gamma}\right)\right]\right\}. \tag{7}$$

Figure 6 shows the dependence of the split phase difference and resonance depth of mode splitting on the coupling parameter when assuming $\gamma = 1/(2^{1/20})$ and $\gamma = 1/(2^{1/2})$. The split phase difference increases from 0 to 2π as K goes from K_{WL_1} to K_{WL_2}, and then continues to the next period. K_{WL_1} and K_{WL_2} are the coupling conditions of the WLC effect condition and correspond to two different orders resonant phases. What is noteworthy is that the resonance splitting difference $\Delta\varphi$

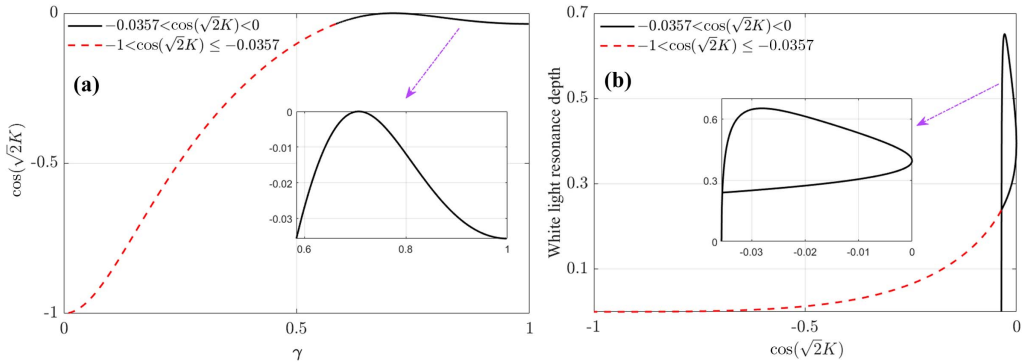

Fig. 5. (a) Coupling state versus loss for achieving the white-light resonance effect and (b) the dependence of white-light resonance depth on the coupling state.

exhibits an approximately exponential evolutionary pattern when the coupling parameter is close to the WLC effect condition K_{WL_1} and K_{WL_2}, and a minute variation in the coupling state can lead to a swift division of the resonance modes in this case. Correspondingly, the resonance splitting difference $\Delta\varphi$ shows an approximately linear trend of evolution in the vicinity of $K = (m + 1/2)\sqrt{2}\pi$. Regrettably, the coupling factor $\cos(\sqrt{2}K) = -1$ in this case, resulting in the MCR being in a detuned state and the resonance depth being reduced to 0. This region of detuning will expand as the degree of loss amplifies. As the loss magnitude is low, the depth of the split mode initially experiences a brief decline and subsequently rises as the coupling state deviates from the condition of the WLC effect. The depth reaches a maximum value at the critical coupling condition of resonance splitting and then decreases again until the splitting mode is detuned at $\cos(\sqrt{2}K) = -1$. For the assumption of $\gamma = 1/(2^{1/20})$, the critical coupling factor of split mode $\cos(\sqrt{2}K_{cri-sp}) = -0.8661$, and the split phase difference is $\Delta\varphi_{cri_1} = 2.3922$ or $\Delta\varphi_{cri_2} = 3.8909$ ($\Delta\varphi_{cri_1} + \Delta\varphi_{cri_2} = 2\pi$) at this point. The depth of the split mode monotonically decreases until detuning as the coupling state away from the condition of the WLC effect when the loss is not less than the critical loss value. When utilizing the MCR at the resonance splitting state for sensing purposes, a trade-off must be made between sensitivity and signal-to-noise ratio. This suggests that the coupling condition under which the operation is performed should be taken into consideration. Figure 6 shows the dependence of the split phase difference and resonance depth of the mode splitting on the coupling parameter when $\gamma = 1/(2^{1/20})$ and $\gamma = 1/(2^{1/2})$, respectively.

5. Conclusions

In conclusion, we have utilized numerical modeling to investigate the periodic evolution of the resonant mode with respect to the coupling state in a three-turn lossy MCR. Under a given loss condition, the resonant mode exhibits periodic evolution among normal resonance, white-light cavity effect, and resonance mode splitting as the change in the phase shift and coupling state. We introduce a coupling factor $\cos(\sqrt{2}K)$ to characterize the coupling state in an MCR. When the coupling state exceeds a certain threshold under a specific loss coefficient, the microfiber coil resonator predominantly exhibits normal resonance with characteristics akin to a single-ring resonator. Once the coupling state decreases to this threshold and matches the loss, the WLC effect will be activated. Moreover, as the coupling state falls below this threshold, the degeneracy of the resonance mode is raised, and the resonant phase undergoes a bifurcation. The excitation conditions for each resonant mode have been derived, and the different critical coupling conditions exist for both normal resonance and mode splitting in the case of relatively small losses. It is found that a threshold loss exists at which the critical coupling states of the normal resonance and mode splitting coincide with the condition of the white-light cavity effect. When the loss exceeds this threshold, the critical coupling conditions for mode splitting will no longer exist. The characteristics of each mode have also been discussed, whereby the feasibility of the WLC effect and resonance splitting by controlling the coupling and loss condition in a three-turn MCR is predicted. These resonance modes have potential applications in fields, such as optical sensing, optical communication, and photonics. The findings presented in this Letter are expected to provide valuable theoretical support for the engineering applications of mode splitting and the WLC effect. A series of experiments will subsequently be conducted to verify the deductions made in this study.

Acknowledgements

This work was supported by the Joint Fund Project (No. 8091B042206), the National Natural Science Foundation of China (No. 61873064), the National Defense Pre-Research Foundation of China (No. 8922006150), the Jiangsu Provincial Key Research and Development Program (No. BE2022139), and the Wuxi Key Research and Development Program (No. N20221003).

References

1. J.-H. Chen, D.-R. Li, and F. Xu, "Optical microfiber sensors: sensing mechanisms, and recent advances," J. Lightwave Technol. **37**, 2577 (2019).
2. J. Zhang, H. Fang, P. Wang, *et al.*, "Optical microfiber or nanofiber: a miniature fiber-optic platform for nanophotonics," Photonics Insights **3**, R02 (2024).
3. M. Sumetsky, "Optical fiber microcoil resonator," Opt. Express **12**, 2303 (2004).
4. C. Alexeyev, S. Aliyeva, E. Barshak, *et al.*, "Slow optical vortices in multicoil fiber resonators," JOSA B **39**, 2289 (2022).
5. H.-J. Yang, Y.-P. Liao, S.-S. Wang, *et al.*, "Analysis of microfiber knot resonator spectrum for seawater temperature," Spectrosc. Spect. Anal. **36**, 2368 (2016).
6. S. Sun, Y. Xu, L. Ren, *et al.*, "Research on the gas refractive index sensing based on microfiber double-knot resonator with a parallel structure," Optik **204**, 164207 (2020).
7. M.-S. Yoon, H.-J. Kim, G. Brambilla, *et al.*, "Development of a small-size embedded optical microfiber coil resonator with high Q," J. Korean Phys. Soc. **61**, 1381 (2012).
8. L. Cai and J. Li, "PDMS packaged microfiber knot resonator used for sensing longitudinal load change," J. Phys. Chem. **138**, 109268 (2020).
9. M. Arjmand, V. Ahmadi, and M. Karimi, "Wavelength-selective optical amplifier based on microfiber coil resonators," J. Lightwave Technol. **30**, 2596 (2012).
10. T. Wang, X. Li, F. Liu, *et al.*, "Enhanced fast light in microfiber ring resonator with a Sagnac loop reflector," Opt. Express **18**, 16156 (2010).
11. Y. Yin, J. Yu, Y. Jiang, *et al.*, "Investigation of temperature dependence of microfibre coil resonators," J. Lightwave Technol. **36**, 4887 (2018).
12. T.-H. Shen and L. A. Wang, "A two-layer microcoil resonator with very high quality factor," IEEE Photonics Technol. Lett. **26**, 535 (2014).
13. A. Kowsari, V. Ahmadi, G. Darvish, *et al.*, "Dynamic analysis of optical microfiber coil resonators," Appl. Opt. **55**, 6680 (2016).
14. Y. Yin, S. Li, J. Ren, *et al.*, "High-sensitivity salinity sensor based on optical microfiber coil resonator," Opt. Express **26**, 34633 (2018).
15. Y. Yin, J. Yu, Y. Jiang, *et al.*, "Investigation of temperature dependence of microfiber coil resonators," J. Lightwave Technol. **36**, 4887 (2018).
16. F. Zhang and X. Chen, "Anomalous optical propagation and potential sensitivity enhancement in a micro-coil resonator based on microfiber," IEEE Photonics J. **13**, 1 (2021).

17. M. Sumetsky, "Uniform coil optical resonator and waveguide: transmission spectrum, eigenmodes, and dispersion relation," Opt. Express **13**, 4331 (2005).
18. J. Scheuer and M. Sumetsky, "Optical-fiber microcoil waveguides and resonators and their applications for interferometry and sensing," Laser Photonics Rev. **5**, 465 (2011).
19. A. Wicht, K. Danzmann, M. Fleischhauer, *et al.*, "White-light cavities, atomic phase coherence, and gravitational wave detectors," Opt. Commun. **134**, 431 (1997).
20. A. Othman, D. Yevick, and M. Al-Amri, "Generation of three wide frequency bands within a single white-light cavity," Phys. Rev. A **97**, 043816 (2018).
21. O. Kotlicki, J. Scheuer, and M. Shahriar, "Theoretical study on Brillouin fiber laser sensor based on white light cavity," Opt. Express **20**, 28234 (2012).
22. Z. Yang, Y. Xiao, J. Huo, *et al.*, "Analysis of nonreciprocal noise based on mode splitting in a high-Q optical microresonator," Laser Phys. **28**, 015101 (2017).
23. C. Ciminelli, C. Campanella, F. Dell'Olio, *et al.*, "Fast light generation through velocity manipulation in two vertically-stacked ring resonators," Opt. Express **18**, 2973 (2010).
24. X. Wang, T. Yuan, J. Wu, *et al.*, "Enhanced temperature sensing by multimode coupling in an on-chip microcavity system," Laser Photonics Rev. **18**, 2300760 (2024).
25. M. Sumetsky, "How thin can a microfiber be and still guide light?" Opt. Lett. **31**, 870 (2006).
26. M. Sumetsky, "Basic elements for microfiber photonics: micro/nanofibers and microfiber coil resonators," J. Lightwave Technol. **26**, 21 (2008).
27. N. G. R. Broderick, "Optical snakes and ladders: dispersion and nonlinearity in microcoil resonators," Opt. Express **16**, 16247 (2008).
28. F. Xu, Q. Wang, J.-F. Zhou, *et al.*, "Dispersion study of optical nanowire microcoil resonators," IEEE J. Sel. Top Quantum Electron. **17**, 1102 (2011).
29. W.-P. Huang and J. Mu, "Complex coupled-mode theory for optical waveguides," Opt. Express **17**, 19134 (2009).
30. Q. Li, T. Wang, Y. Su, *et al.*, "Coupled mode theory analysis of mode-splitting in coupled cavity system," Opt. Express **18**, 8367 (2010).